

Pressure induced topochemical polymerization of solid acrylamide facilitated by anisotropic response of hydrogen bond network

Supplementary Information

Sayan Maity,[†] Abhijeet S. Gangan,[‡] Ashwini Anshu,[†] Rashid Rafeek V.
Valappil,[†] Brahmananda Chakraborty,^{‡,¶} Lavanya M. Ramaniah,^{*,‡,¶} and
Varadharajan Srinivasan^{*,†}

[†]*Department of Chemistry, Indian Institute of Science Education and Research Bhopal,
Bhopal 462 066, India*

[‡]*High Pressure and Synchrotron Radiation Physics Division, Bhabha Atomic Research
Centre, Trombay, Mumbai 400085, India*

[¶]*Homi Bhabha National Institute, Mumbai 400094, India*

E-mail: lavanya@barc.gov.in; vardha@iiserb.ac.in

Cell optimization details

Compression optimization

In order to obtain the structure of the polymer, cell optimizations are started from the unpolymerized structures at first. Starting from 0 GPa structure, pressure was increased step by step with 2 GPa increment and cell optimizations were performed at each pressure starting from the optimal structure in the previous step. By this method, a polymer structure was obtained at 102 GPa, due to the formation of new C-C and C-O bonds. Thus, at 102 GPa, existence of any unpolymerized structure as a minimum in potential energy surface was ruled out. Mechanical stability of this polymer was checked by performing phonon analysis which is described later.

Decompression optimization

After noting the structural features and bond connectivity of the possible polymer at 102 GPa, starting from that structure, optimizations were performed at lower pressures step by step, with 2 GPa decrement. This resulted in polymers with exactly same bond connectivity from 100 GPa down to 0 GPa, which are mechanically stable (as validated by phonon analysis). Thus, it was confirmed that, from 0 to 100 GPa, both the polymerized and unpolymerized structures are minima in potential energy surface. Comparison of the enthalpy of both structures at each pressure revealed that from 0 to 22 GPa, the unpolymerized structures have the lower enthalpy, whereas from 24 GPa, the enthalpy of the polymerized minima become lower than the unpolymerized ones. Thus, it was confirmed the polymerized form of acrylamide becomes thermodynamically more stable at and beyond 24 GPa. i.e. this is the first-order transition pressure.

Optimizations at lower pressures, starting from 102 GPa entail an increase in the cell volume. In such cases, it is worth mentioning that accurate computation of stresses and prediction of structures requires large plane-wave basis set cutoffs.¹ Thus, convergence in

energies, forces as well as stresses with respect to the basis set size, set by kinetic energy cut-off have to be ensured, which have been well tested in our calculations. The usage of 62 Ry and 480 Ry of kinetic energy cut-off and charge density cut-off, achieves the convergence of energy, forces and components of stress within 10^{-8} Ry, 10^{-5} Ry/Bohr and 0.5 kbar, respectively, thus providing the required accuracy.

Structural data

The calculated bond lengths and bond angles of *s-cis* conformer of acrylamide molecule (gas phase) are given in Table S1. The corresponding experimental values from the literature are also given (in parentheses) for comparison.

Table S1: Bond lengths and bond angles of *s-cis* conformer of acrylamide molecule (gas phase). The experimental values from the literature² are given in parentheses for comparison.

Bond type	Bond length (Å)	Bond angle type	Bond angle (°)
N-H	1.021 (1.01)	H-N-H	119.199 (118.0)
N-C	1.374 (1.38)	N-C-O	122.045 (122.1)
C-O	1.234 (1.22)	O-C-C	123.513 (123.3)
C-C	1.497 (1.50)	H-C-H	118.665 (118.2)
C-H	1.102 (1.09)	N-C-C	114.442 (114.6)
C=C	1.337 (1.33)		

The geometry optimized lattice parameters at 0 GPa, for acrylamide crystal, calculated using three different functionals - the local density approximation (LDA), the generalised gradient approximation (GGA) and GGA+ van der Waals (vdW) - are given in Table S2. For the purpose of benchmarking, van der Waals corrections due to Grimme’s DFT-D2³ (D2), Tkatchenko-Scheffler⁴ (TS) and the exchange-correlation functional due to Thonhauser *et al.*⁵, vdW-DF2 (DF2), are compared.

Experimental values from the literature are also given. It is clear that the best agreement with the experiment come from the various types of GGA+vdW. At various pressures, a

Table S2: Lattice parameters calculated using different functionals at ambient pressure. The experimental values from the literature are given for comparison.

lattice parameters	Theory					Experiment ⁸
	LDA ⁶	GGA ⁷	GGA+D2 ³	GGA+TS ⁴	DF2 ⁵	
a (Å)	7.212	8.219	7.995	7.858	8.214	8.228
b (Å)	5.759	6.971	5.746	5.757	5.753	5.759
c (Å)	9.433	9.708	9.661	9.742	9.945	9.76
β (°)	118.346	116.569	122.405	119.246	120.905	120.04
Volume (Å ³)	345.855	497.54	374.737	384.559	403.251	400.3

comparison of the lattice parameters obtained using D2, TS and vdW-DF2 corrections, (see Figure S1(a)) shows there are negligible differences between them. Also, the comparison of various hydrogen bond parameters and intermolecular distances due to these functionals are given in Figure S1(b) and Figure S1(c). The D2 functional was preferred for all the calculations reported in this work, since it involves a lower computational expense. It is to be noted that, all the important structural changes are reproduced well with the other vdW functionals.

The evolution of the lattice parameters and monoclinic angle with pressure, up to 102 GPa, are given in Figure S1(d). Noticeable changes occur around two pressures : at ~ 4 GPa, attributable to the slight reorientation in the H-bonding network; and at ~ 24 GPa, attributable to polymerization.

The evolution of the intramolecular bonding distances C1=C2, C2-C3, C3=O, C3-N with pressure, up to 102 GPa, are given in Figure S2(a). It is seen from the figure that at ~ 24 GPa, C1=C2 and C3=O double bonds become single bonds. C2-C3 and C3-N both get shortened with pressure, but at ~ 24 GPa they assume values close to the ambient pressure values. The C=O \cdots H-N dihedral angle for the inter-dimer H-bond shows change in sign (see Figure S2(b)) at ~ 4 and ~ 12 GPa, indicating orientational transitions in the H-bond network at these pressures. The evolution of the angle between two dimer rows (θ) existing in a sheet, with pressure, is shown in Figure S2(c).

At ~ 24 GPa, inter-sheet C2'-C2'' and C1-O' bond formation occurs along the a and

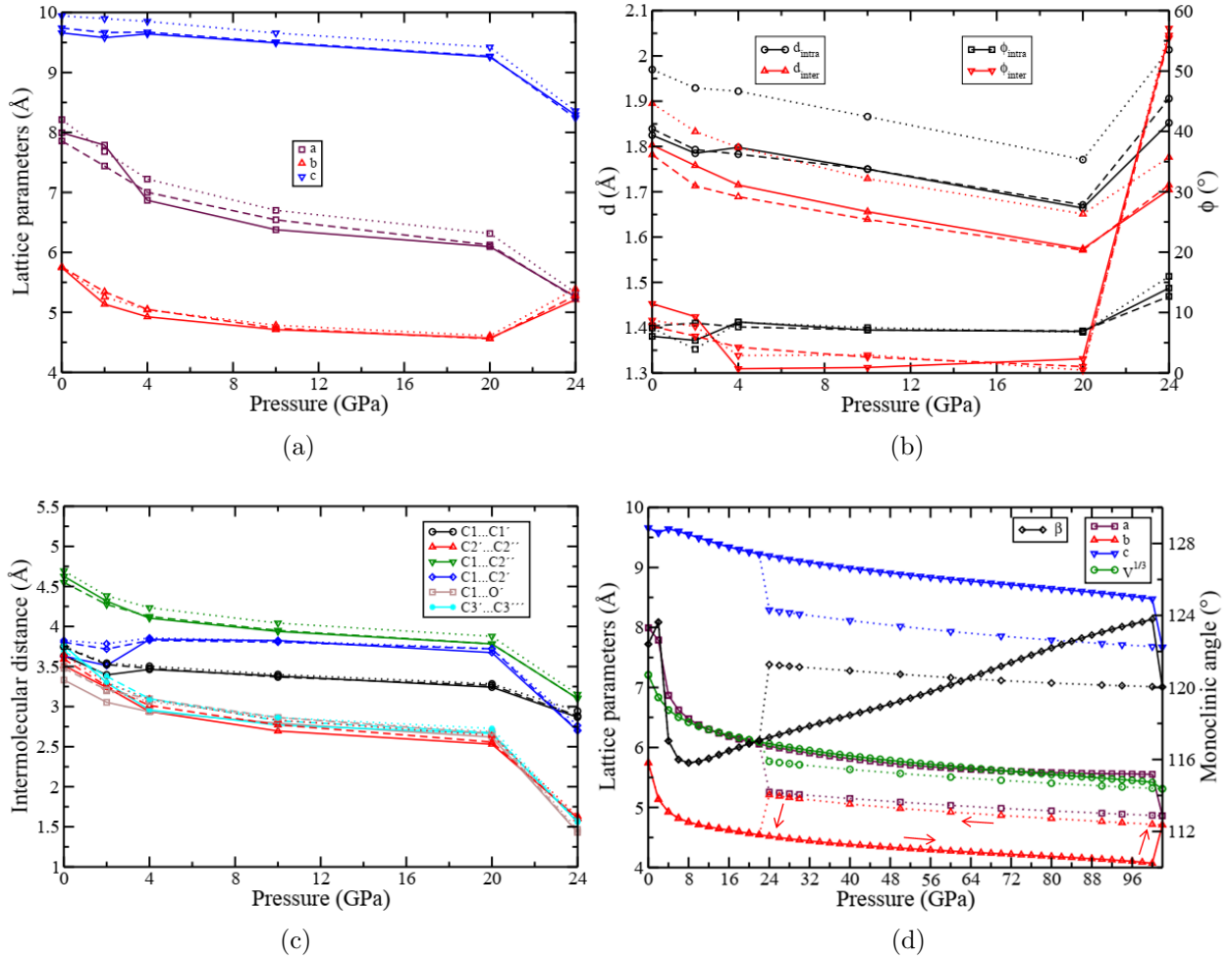


Figure S1: Comparison of (a) lattice parameters (b) hydrogen bond lengths (d) and distortions (ϕ) (c) intermolecular distances, using D2, TS and DF2 functionals. Lines are drawn as guides to the eye. Continuous lines are for D2, dashed lines are for TS and dotted lines are for DF2. (d) Evolution of lattice parameters with pressure using D2 functional. The arrows indicate the optimization sequence used to obtain the structures and the dotted lines (branching off from 22 GPa) correspond to the structures which have lowest enthalpy at the corresponding pressures.

c directions, respectively, whereas intra-sheet $C3'-C3'''$ bond formation occurs along the a direction. These can be seen from the Figure S3(a) and S3(b).

The structural parameters of the polymers at 0 GPa and 24 GPa obtained by decompression optimizations are compared in Table S3. The charge density of the dynamically stable polymers at both these pressures are also shown in Figure S4.

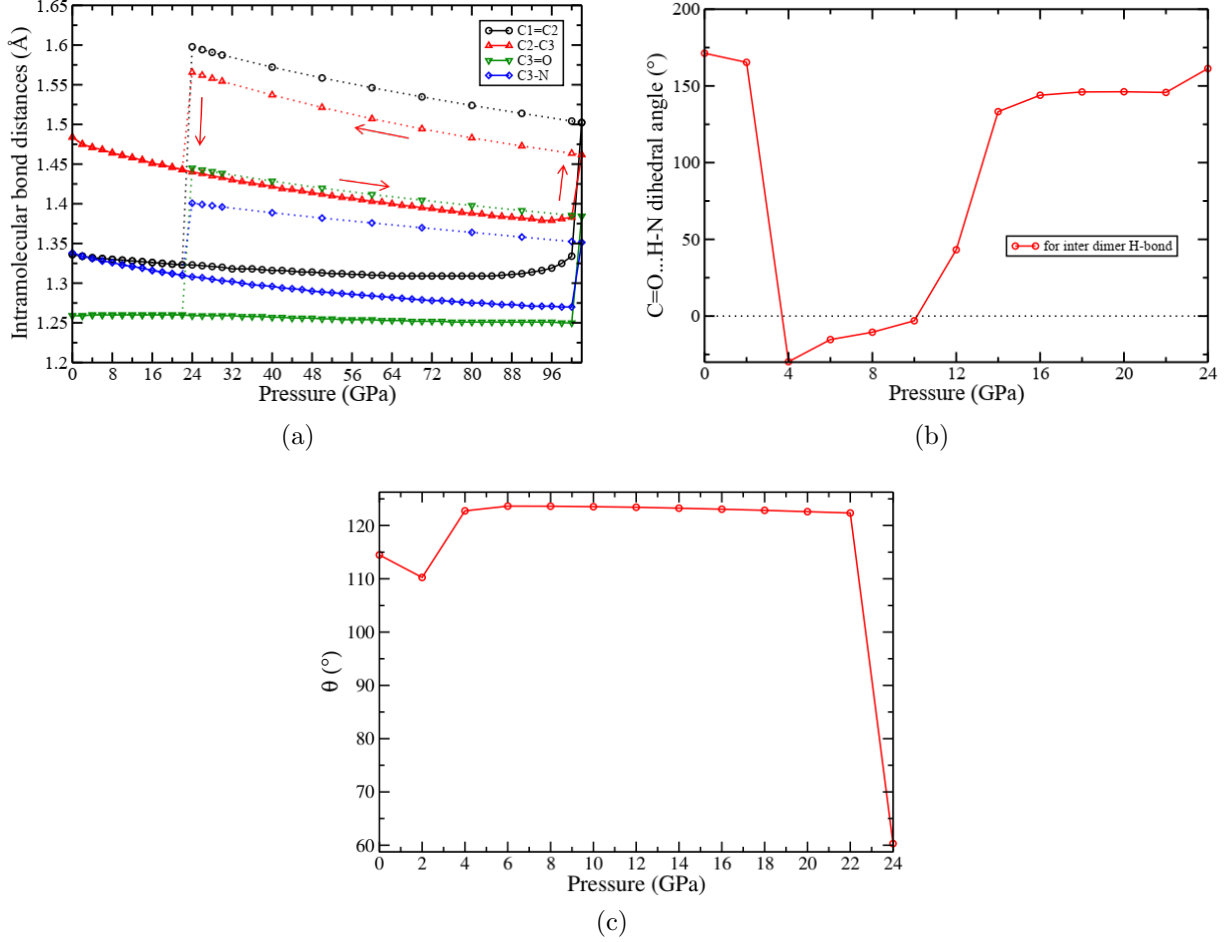


Figure S2: (a) Evolution of intramolecular bonding distances with pressure. The dotted lines from 22 GPa correspond to the structures which have lowest enthalpy and the arrows indicate the optimization pathway; (b) Evolution of C=O...H-N dihedral angle associated with inter dimer H-bond; (c) Evolution of θ (dihedral angle of C2-C3-C3'-C2') with pressure. The 24 GPa data-points in (b) and (c) are for the polymer whereas the others are unpolymerized.

Table S3: Structural parameters of polymerized structures at both 0 GPa and 24 GPa

Lattice parameters	0 GPa	24 GPa	Bond lengths	0 GPa	24 GPa
a (Å)	5.512	5.258	C1=C2 (Å)	1.655	1.598
b (Å)	5.695	5.211	C2-C3 (Å)	1.628	1.566
c (Å)	8.664	8.291	C3=O (Å)	1.483	1.445
β (°)	122.197	122.271	C3-N (Å)	1.418	1.401

Phonon data

Pressure dependence of vibrational frequencies and IR intensities

The IR and Raman modes calculated at 0 GPa were identified and match well with experiment in the region of 600–3800 cm^{-1} . These ⁶ are given in Table S4. The evolution of the IR

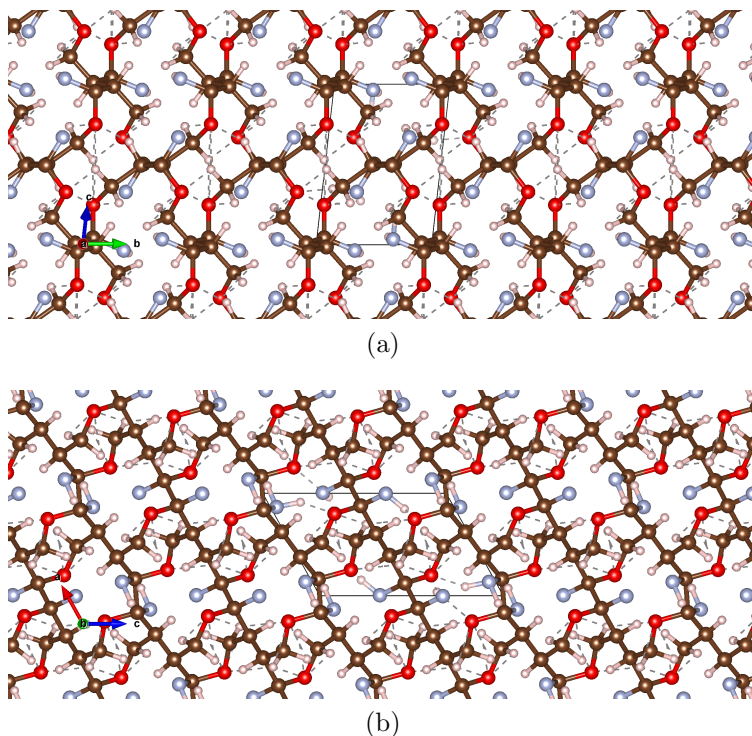


Figure S3: Structure of acrylamide polymer at 24 GPa, as seen (a) along the a axis, and (b) along the b axis. Red spheres represent O, brown C, grey N and light pink H atoms, respectively.

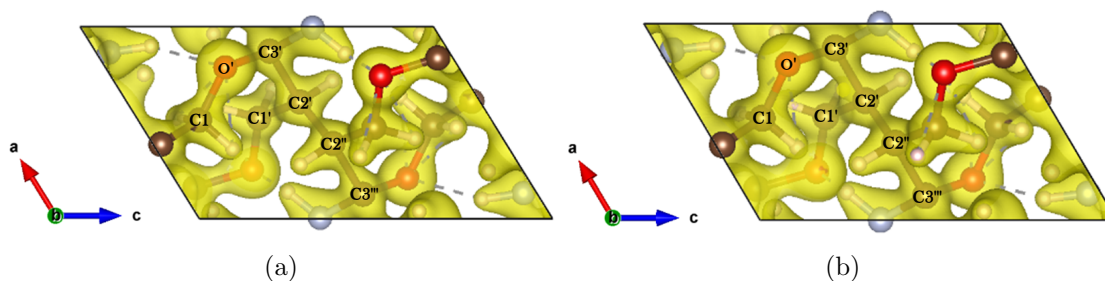


Figure S4: Charge density of acrylamide polymer obtained by decompression optimizations at (a) 0 GPa; and (b) 24 GPa. Red spheres represent O, brown C, grey N and light pink H atoms, respectively.

spectra in the high frequency region with pressure is given in Figure S5. The most significant trends observed in our calculations have been discussed in the main text.

In the experimental IR and Raman spectra, the increase in intensity and spread of stretching CH and CH₂ peaks at ~ 17 GPa were correlated with polymerization.^{9,10} In the calculated IR spectra, at ~ 14 GPa, those intensities increase, and the occurrence of closely spaced mul-

Table S4: Comparison of different IR and Raman active modes with experiment at 0 GPa. γ -rocking, t -twisting, ω -wagging, δ -deformation, $\$$ -scissoring, ν -stretching, τ -torsion

Mode type	IR Mode (cm ⁻¹)		Raman Mode (cm ⁻¹)	
	Theory	Experiment	Theory	Experiment
δ -CC	322.32, 324.98	-	304.22, 312.76	300(δ -C=C-C) ⁹
γ -CC + γ -CO	619.58, 624.69	626 (γ -CC) ^{10,11}	605.02, 617.15	626 (γ -CC) ^{9,11}
ω -NH ₂	723.30, 753.89	708(t -NH ₂) ^{10,11}	728.70, 760.02	708 (t -NH ₂) ¹¹
τ -CC	791.25, 804.79	-	796.73, 799.14	-
t -NH ₂ + ν -CC	862.53, 871.07	-	829.39, 839.71, 856.64	-
τ -CC	791.25, 804.79	-	796.73, 799.14	-
ν -CC + δ -NH ₂	843.01, 852.61	841 (ν -CC) ¹²	837.28	-
ω -CH ₂	955.24, 957.60	962 (ω -CH ₂) ¹⁰	954.11, 957.24	962 (ω -CH ₂) ⁹
γ -CH ₂ + CH	1035.82, 1040.75	1053 (γ -CH ₂) ¹¹ 1051 (CH ₂) ¹²	1037.39, 1042.09	1052 (γ -CH ₂) ^{9,11}
γ -NH ₂ + CO	1148.14, 1155.22	1137 (γ -NH ₂) ¹²	1160.11, 1161.89	-
γ -CH + δ -CH ₂	1272.93, 1278.43	1281 (γ -CH) ¹²	1275.04, 1280.69	-
$\$$ -CH ₂ + ν -CN	1350.4, 1356.86	1353 (ν -CN) ¹²	1353.75, 1364.00	-
δ -CH ₂ + ν -C-C + ν -CN	1417.70, 1419.97	1430 (ν -CN) ¹¹ 1429 (δ -CH ₂) ¹² 1430 (ν -CN/ δ -CH ₂) ¹⁰	1426.45, 1436.47	1432 (ν -CN) ¹¹ 1432 (ν -CN/ δ -CH ₂) ⁹
ν -CC + $\$$ -NH ₂	1636.69, 1635.63, 1661.85	1650 (ν -CC) ¹¹ 1648 (ν -CC) ¹² 1650 (ν -CC) ¹⁰	1644.41, 1645.50	1639 (ν -CC) ^{9,11}
ν -CO + $\$$ -NH ₂	1696.85	1675 (ν -CO) ¹¹ 1674 (ν -CO) ¹²	1664.60, 1664.50	1680 (ν -CO) ^{9,11} 1685 (ν -CO) ¹¹
ν_s -CH ₂	3070.34, 3069.51		3070.32, 3069.35	3036 (ν_s -CH ₂) ⁹
ν -CH	3095.23, 3095.52		3097.18, 3097.73	3013 (ν -CH) ⁹
ν_s -NH ₂	3146.55	3187 (ν_s -NH ₂) ¹⁰	3125.41, 3131.97	3165 (ν_s -NH ₂) ⁹
ν_{as} -CH ₂	3176.89, 3177.03		3176.79, 3177.48	3105 (ν_{as} -CH ₂) ⁹
ν_{as} -NH ₂	3182.02, 3312.95, 3302.05	3352 (ν_{as} -NH ₂) ¹⁰	3337.75, 3287.43	3335 (ν_{as} -NH ₂) ⁹

multiple CH and CH₂ modes leads to the increase in spread of these modes. This may be due to the change in the electronic environment at ~ 14 GPa, however, no polymerization is seen in our calculations at these pressures.

Phonon dispersion and density of states

Figure S7(a) and S7(b) show the phonon dispersions for unpolymerized acrylamide crystal at 0 GPa and 22 GPa, whereas Figure S7(c) and S7(d) show the dispersions of acrylamide polymer at 24 GPa and 102 GPa. The phonon dispersions were calculated along paths joining high-symmetry q -points in the first Brillouin zone (BZ) of the appropriate Bravais lattice as

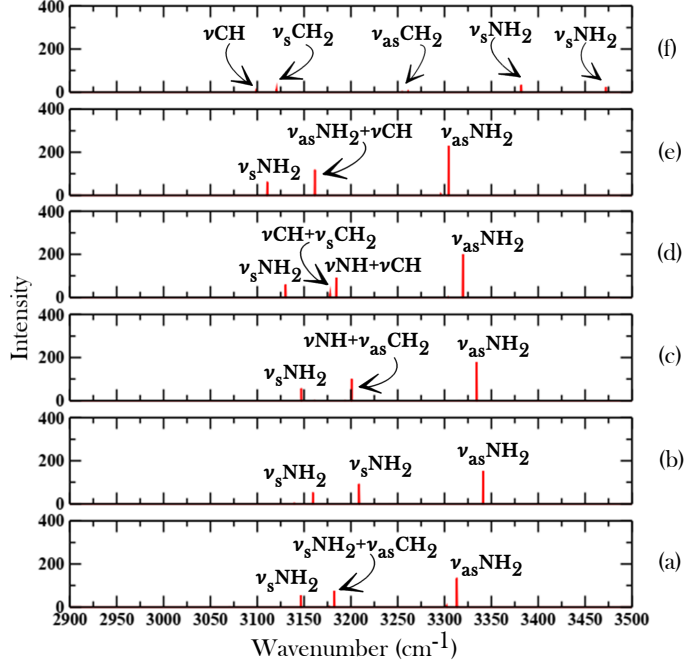


Figure S5: IR spectra of acrylamide in high frequency region at (a) 0 GPa; (b) 4 GPa; (c) 10 GPa; (d) 14 GPa; (e) 20 GPa; and (f) 24 GPa. The 24 GPa panel is for polymerized structure while the rests are for unpolymerized structures.

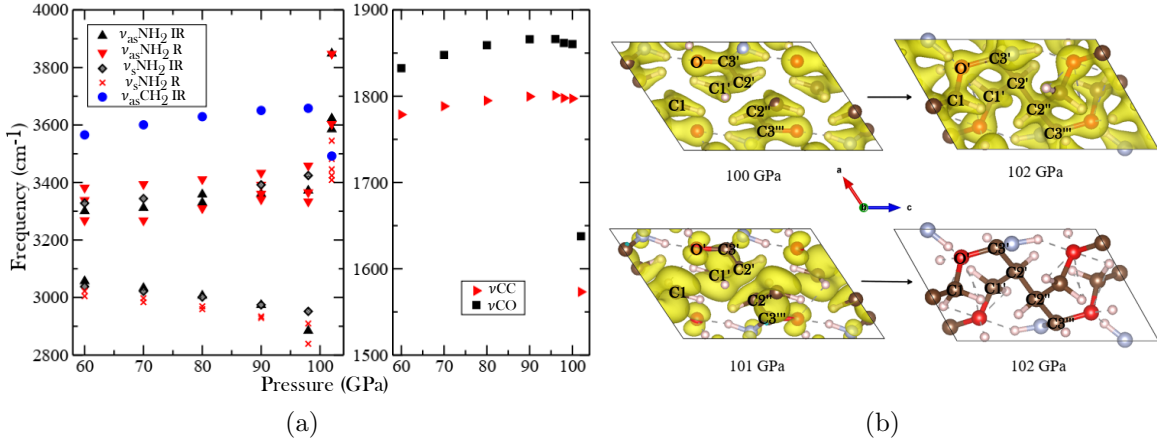


Figure S6: (a) Evolution of all Raman and IR active νNH_2 , νCH_2 modes (left) and IR active $\nu\text{C}=\text{C}$, $\nu\text{C}=\text{O}$ modes (right) in the high pressure range; (b) Charge density (top panel) and spin density plots just before and at the polymerization pressure. All of these plots are for metastable structures except 102 GPa.

described by Hinuma *et al.*¹³ Soft phonon modes with imaginary frequencies are associated with dynamical instability.¹⁴ The absence of any imaginary frequencies throughout the entire BZ in these plots confirms the dynamical stability of the structures at the aforementioned

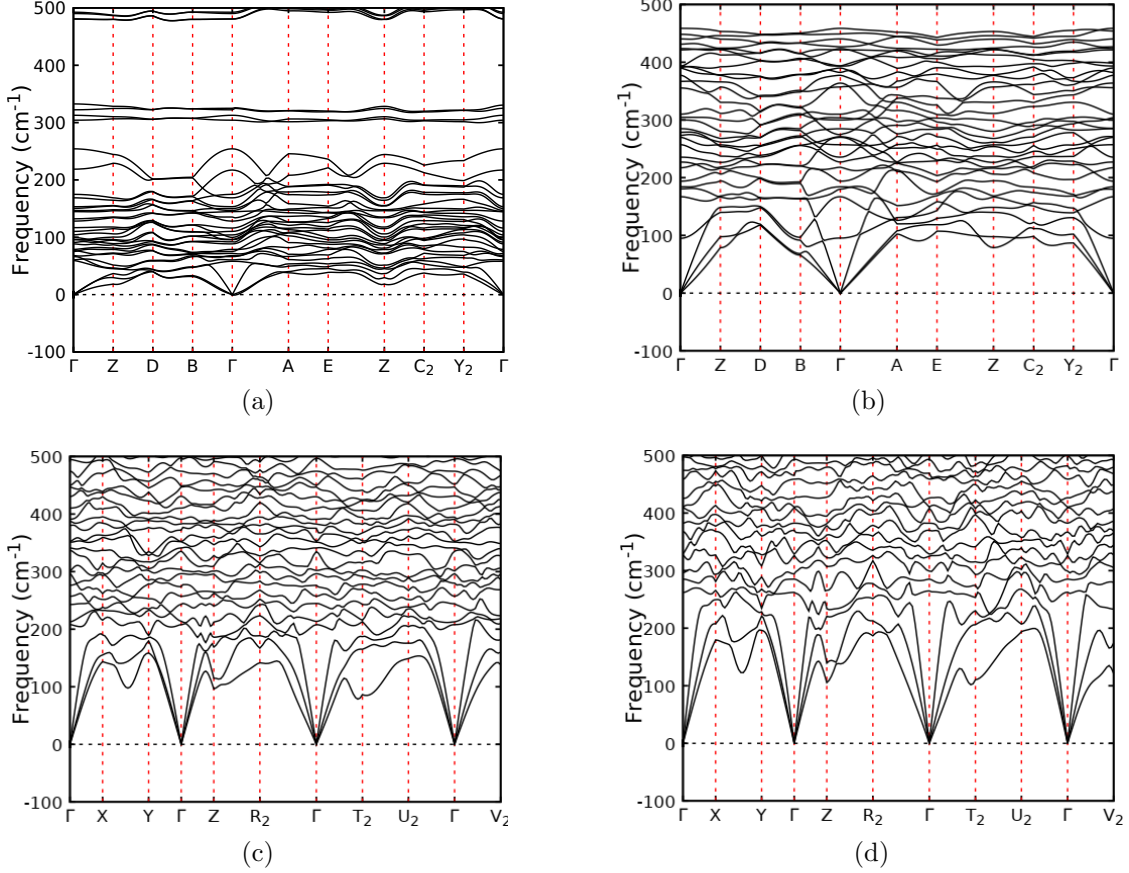


Figure S7: Phonon dispersions at (a) 0 GPa (unpolymerized); (b) 22 GPa (unpolymerized); (c) 24 GPa (polymerized) and (d) 102 GPa (polymerized).

pressures.

The partial phonon density of states (PhDOS) for acrylamide crystal at 0 GPa is given in Fig. S8(a), and for the polymeric phase at 24 GPa in Figure S8(b)–(d). In the PhDOS, the maximum contribution over the frequency range $\sim 3200\text{ cm}^{-1}$ to $\sim 3600\text{ cm}^{-1}$, is from hydrogen because of its low atomic mass. At $\sim 3676\text{ cm}^{-1}$, at 24 GPa, the contribution of nitrogen and hydrogen to the PhDOS is due to NH_2 vibrations, which are not present at ambient pressure. This implies the occurrence of a new hydrogen bonded framework at 24 GPa, which is consistent with our structural and spectral studies. Normally $\text{C}=\text{O}$ and $\text{C}=\text{C}$ vibrational frequencies lie between $\sim 1650\text{ cm}^{-1}$ to $\sim 1700\text{ cm}^{-1}$. However, the absence of oxygen, and fewer carbon states in the same region as well as the shifting of those states to the lower frequency region in the PhDOS plot, also indicate transformation of the $\text{C}=\text{O}$

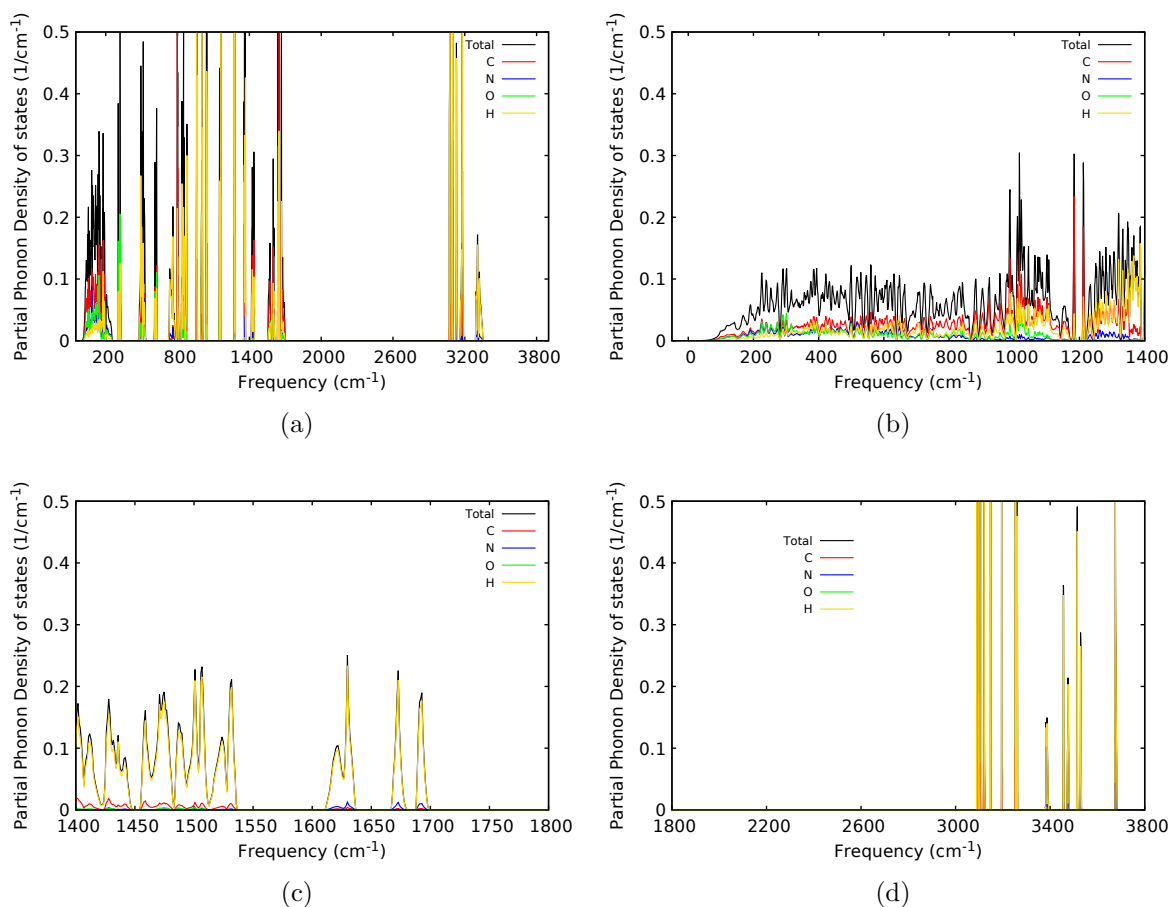


Figure S8: Partial phonon DOS : (a) at 0 GPa (unpolymerized); and at 24 GPa (polymerized) in the (b) low, (c) mid, and (d) high frequency region.

and C=C double bonds into single bonds. These observations are also consistent with the structural changes derived from the atomistic parameters and calculated spectral data.

Electronic Structure

The electronic structure calculations at 0 GPa show that acrylamide crystal is an insulator with a band gap of 3.63 eV. The nature of the band gap is indirect, as the valence band maximum (VBM) lies at the Z symmetry point as shown in Figure S9(a), and the conduction band minimum (CBM) is off the Z point in the direction $(0.0, 0.0, 0.0) \rightarrow (0.0, 0.5, 0.0)$. The bands in the BZ are quite flat at 0 GPa as expected for a molecular crystal. In the polymer

at 24 GPa, the band gap becomes 4.52 eV and is still indirect, and the VBM and CBM lie near the Γ point (see Figure S9(b)).

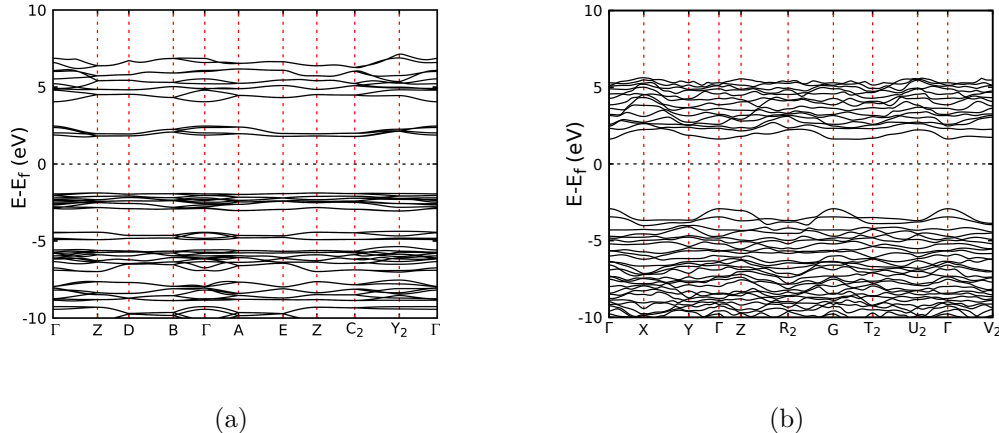


Figure S9: Band structure of acrylamide crystal at (a) 0 GPa (unpolymerized); and (b) 24 GPa (polymerized).

Upon investigating the partial density of states (PDOS) at 0 GPa (see Figure S10(a)), one can infer that the VBM is dominated by the oxygen p states, followed by the carbon and nitrogen p states. The main contribution to these states is from the lone pairs of oxygen and nitrogen. At 24 GPa, the lone pairs of oxygen are shifted away from the Fermi level, implying their participation in bonding; whereas the presence of nitrogen p states closer to the Fermi level than the other states indicates that nitrogen lone pairs stay intact (see Figure S10(b)).

In the compression optimization path at 101 GPa, right before the polymerization occurs, radicals are formed on C1, C2, C3, O and N, (see Figure S6(b)) resulting in differences in the DOS in spin-up and spin-down channels (see Figure S10(d)) and signaling the proximity to an electronic instability. They participate in making C1-O', C2'-C2'' and C3'-C3'''. The formation of the C3'-C3''' bond happens by a radical which is delocalized on the C3-N bond. The partial density of states at 102 GPa is shown in Figure S10(c).

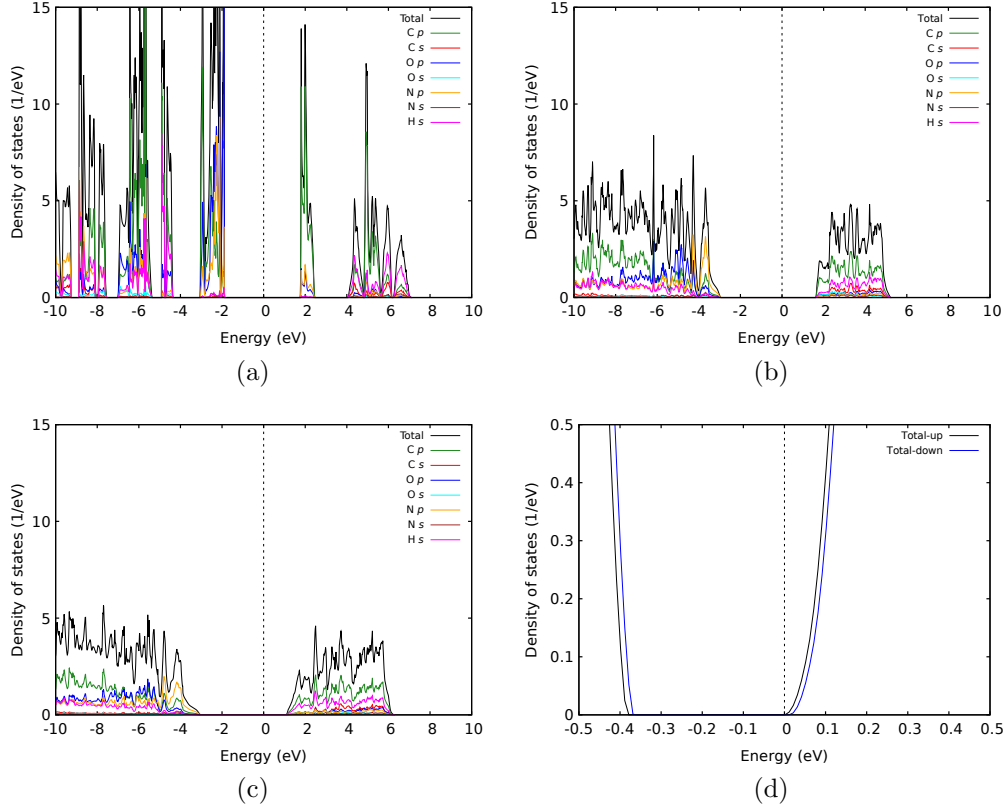


Figure S10: Partial density of states of acrylamide polymer at (a) 0 GPa (unpolymerized); (b) 24 GPa (polymerized); (c) 102 GPa (polymerized); and (d) total density of states at 101 GPa (unpolymerized)

Effect of Temperature

Transformation into polymer from unpolymerized structure at various pressures depend on two factors: (1) activation barrier, and (2) the thermally induced fluctuations of distance between two sp^3 centers which connect upon polymerization. Accounting for both of the factors a simplified model is developed to calculate the rate of polymerization at any temperature-pressure, which is described below in detail.

The fluctuations between two atoms which are polymerizing centers i and j (for example C1-O', C2'...C2'', C3'...C3''') in the unit cell consisting N_a atoms, at temperature T and pressure P , are denoted as $\sigma_{ij}(T, P)$. Using Γ point frequencies ω_k and displacements of atoms (\vec{u}_{ik} , \vec{u}_{jk}) associated with k -th normal mode of the unpolymerized structure at 0 K

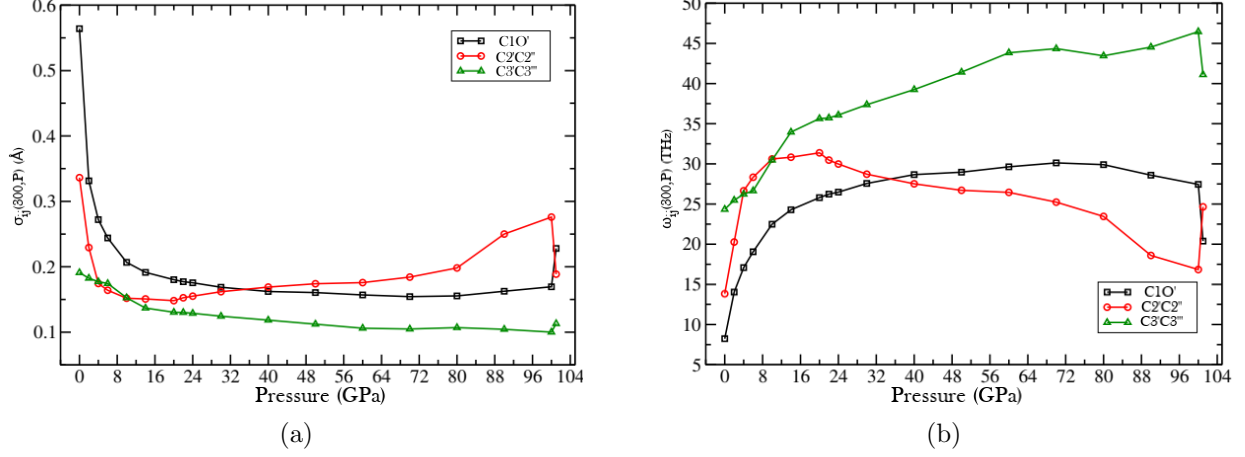


Figure S11: (a) $\sigma_{ij}(300, P)$, Fluctuations of C1...O', C2'...C2'' and C3'...C3''' at 300 K; (b) $\omega_{ij}(300, P)$, Frequency of fluctuations of C1...O', C2'...C2'' and C3'...C3''' at 300 K.

and pressure P , the fluctuations along the vector \hat{r}_{ij} joining two atoms with mass of M_i and M_j can be calculated as follows:^{15,16}

$$\sigma_{ij}(T, P)^2 = \frac{2\hbar}{N_a} \sum_{k=1}^N \frac{1}{\omega_k} \left(\langle n_k \rangle + \frac{1}{2} \right) \left[\frac{1}{2} \left\{ \frac{|\vec{u}_{ik} \cdot \hat{r}_{ij}|^2}{M_i} + \frac{|\vec{u}_{jk} \cdot \hat{r}_{ij}|^2}{M_j} \right\} - \frac{|\vec{u}_{ik} \cdot \hat{r}_{ij}| |\vec{u}_{jk} \cdot \hat{r}_{ij}|}{\sqrt{M_i M_j}} \right] \quad (1)$$

Here $\langle n_k \rangle$ is the expectation value of phonon number operator ($\langle n_k \rangle = \frac{1}{e^{\hbar\omega_k/k_B T} - 1}$).

The values of $\sigma_{C1O'}(T, P)$ increase with temperature (at a constant P) as displacement should increase with temperature. But they decrease with pressure (at a constant T) as, in more compact environment, at high pressures, displacement of atoms become less. At 300 K, rapid changes in the fluctuation in the region 2-4 GPa and 100-101 GPa are observed due to the H-bond reorientation and the change in electronic structure, respectively (see Figure S11(a)).

The rate of a reaction or transformation from unpolymerized structure to the polymer can be written following Arrhenius equation:

$$r_{u \rightarrow p, ij}(T, P) = \omega_{ij}(T, P) \exp \left\{ -\frac{E_{u \rightarrow p, ij}^a}{kT} \right\} \quad (2)$$

As mentioned previously there are three possible pairs of i and j related to new bond

formation towards polymerization. $\omega_{ij}(T, P)$ is the frequency of fluctuations between those atoms. It accounts for the atomic orientations which could be favourable for new bond formation. This is calculated in the classical limit:

$$\omega_{ij}(T, P) = \sqrt{\frac{k_B T}{\mu_{ij} \sigma_{ij}(T, P)^2}} \quad (3)$$

At 300K, the frequencies of fluctuations corresponding to all possible pairs of atoms depict rapid changes in the region 1-2 GPa and 100-101 GPa due to the similar reasons described earlier (see Figure S11(b)).

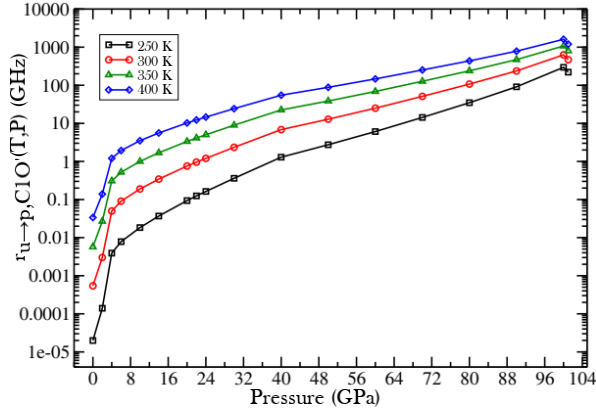
$E_{u \rightarrow p, ij}^a$ is the activation barrier for the bond formation between i and j which can be approximated as activation barrier from unpolymerized to completely polymerized (all three types of bonds are formed) structure and equation (6) is rewritten as:

$$r_{u \rightarrow p, ij}(T, P) = \omega_{ij}(T, P) \exp \left\{ -\frac{E_{u \rightarrow p}^a}{kT} \right\} \quad (4)$$

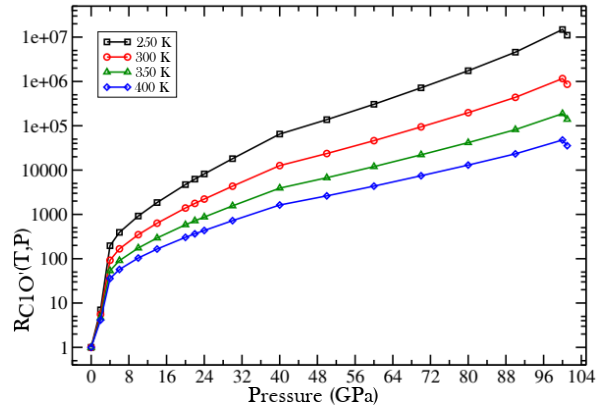
The relative rate of reaction is defined as:

$$R_{ij}(T, P) = r_{u \rightarrow p, ij}(T, P) / r_{u \rightarrow p, ij}(T, 0) \quad (5)$$

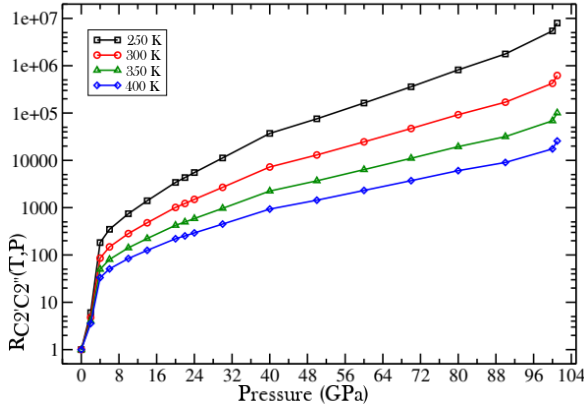
The absolute and relative rates (with respect to the rate at 0 GPa) of reaction are calculated from the above mentioned equations. The absolute rate of C1...O' increases with temperature and pressure, individually (see Figure S12(a)). The relative rates calculated at different temperatures for C1...O', C2'...C2'' and C3'...C3''' atom pairs are shown in Figure S12(b)-(d). In all these plots, the rates increase rapidly up to 4 GPa due to the sudden decrease of enthalpy barrier, as a consequence of H-bond reorientation. After 4 GPa, the rates increase rather slowly. Overall, the increase of rates with pressure suggests that, even at room temperature polymerization reaction at 24 GPa will be significantly slower than much higher pressure.



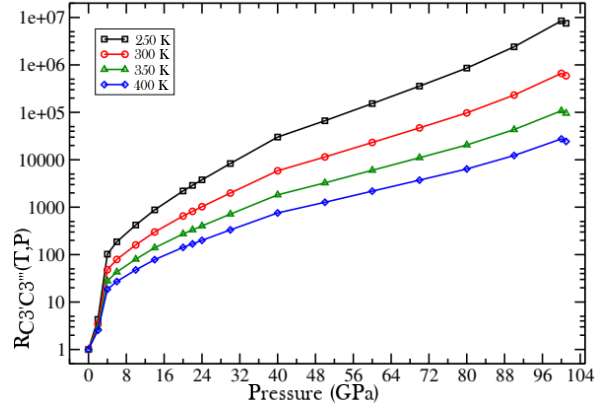
(a)



(b)



(c)



(d)

Figure S12: (a) Absolute rate of C1...O' bond formation, $r_{u \rightarrow p, C1O'}(T, P)$; (b) Relative rate of C1...O' bond formation, $R_{C1O'}(T, P)$; (c) Relative rate of C2'...C2'' bond formation, $R_{C2'C2''}(T, P)$; and (d) Relative rate of C3'...C3''' bond formation, $R_{C3'C3'''}(T, P)$.

References

- (1) Dacosta, P. G.; Nielsen, O.; Kunc, K. Stress theorem in the determination of static equilibrium by the density functional method. *Journal of Physics C: Solid State Physics* **1986**, *19*, 3163.
- (2) Duarte, A.; da Costa, A. A.; Amado, A. On the conformation of neat acrylamide dimers - a study by ab initio calculations and vibrational spectroscopy. *Journal of Molecular Structure: Theochem* **2005**, *723*, 63 – 68.
- (3) Grimme, S. Semiempirical GGA-type density functional constructed with a long-range dispersion correction. *Journal of Computational Chemistry* **2006**, *27*, 1787–1799.
- (4) Tkatchenko, A.; Scheffler, M. Accurate molecular van der Waals interactions from ground-state electron density and free-atom reference data. *Physical review letters* **2009**, *102*, 073005.
- (5) Thonhauser, T.; Cooper, V. R.; Li, S.; Puzder, A.; Hyldgaard, P.; Langreth, D. C. Van der Waals density functional: Self-consistent potential and the nature of the van der Waals bond. *Physical Review B* **2007**, *76*, 125112.
- (6) Perdew, J. P.; Wang, Y. Accurate and simple analytic representation of the electron-gas correlation energy. *Phys. Rev. B* **1992**, *45*, 13244–13249.
- (7) Perdew, J. P.; Burke, K.; Ernzerhof, M. Generalized Gradient Approximation Made Simple. *Phys. Rev. Lett.* **1996**, *77*, 3865–3868.
- (8) Udovenko, A. A.; Kolzunova, L. G. Crystal structure of acrylamide. *Journal of Structural Chemistry* **2008**, *49*, 961–964.
- (9) Sharma, B. B.; Murli, C.; Sharma, S. M. Hydrogen bonds and polymerization in acrylamide under pressure. *Journal of Raman Spectroscopy* **2013**, *44*, 785–790.

- (10) Bhatt, H.; Deo, M. A synchrotron infrared absorption study of pressure induced polymerization of acrylamide. *Spectrochimica Acta Part A: Molecular and Biomolecular Spectroscopy* **2017**, *185*, 45 – 51.
- (11) Murugan, R.; Mohan, S.; Bigotto, A. FTIR and polarised Raman spectra of acrylamide and polyacrylamide. *J. Korean Phys. Soc* **1998**, *32*, 505–512.
- (12) Šimon, E. K.-P. Š.-P.; Gatial, A. Confirmation of polymerisation effects of sodium chloride and its additives on acrylamide by infrared spectrometry. *Journal of Food and Nutrition Research* **2007**, *46*, 39–44.
- (13) Hinuma, Y.; Pizzi, G.; Kumagai, Y.; Oba, F.; Tanaka, I. Band structure diagram paths based on crystallography. *Computational Materials Science* **2017**, *128*, 140 – 184.
- (14) Parlinski, K.; Li, Z. Q.; Kawazoe, Y. First-Principles Determination of the Soft Mode in Cubic ZrO₂. *Phys. Rev. Lett.* **1997**, *78*, 4063–4066.
- (15) Chung, J. S.; Thorpe, M. Local atomic structure of semiconductor alloys using pair distribution functions. *Physical Review B* **1997**, *55*, 1545.
- (16) Togo, A.; Tanaka, I. First principles phonon calculations in materials science. *Scripta Materialia* **2015**, *108*, 1–5.